

Document downloaded from:

<http://hdl.handle.net/10251/80985>

This paper must be cited as:

Galindo, J.; Ruiz Rosales, S.; Dolz Ruiz, V.; Royo-Pascual, L. (2016). Advanced exergy analysis for a bottoming organic rankine cycle coupled to an internal combustion engine. *Energy Conversion and Management*. 126:217-227. doi:10.1016/j.enconman.2016.07.080.



The final publication is available at

<http://dx.doi.org/10.1016/j.enconman.2016.07.080>

Copyright Elsevier

Additional Information

1 **ADVANCED EXERGY ANALYSIS FOR A BOTTOMING ORGANIC**
2 **RANKINE CYCLE COUPLED TO AN INTERNAL COMBUSTION**
3 **ENGINE**

4 **J. Galindo, S. Ruiz, V. Dolz¹, L. Royo-Pascual**

5 CMT – Motores Térmicos, Universitat Politècnica de València, Spain

6 **Abstract**

7 This paper deals with the evaluation and analysis of a bottoming ORC cycle
8 coupled to an IC engine by means of conventional and advanced exergy analysis.
9 Using experimental data of an ORC coupled to a 2 l turbocharged engine, both
10 conventional and advanced exergy analysis are carried out. Splitting the exergy
11 in the advanced exergy analysis into unavoidable and avoidable provides a
12 measure of the potential of improving the efficiency of this component. On the
13 other hand, splitting the exergy into endogenous and exogenous provides
14 information between interactions among system components. The result of this
15 study shows that there is a high potential of improvement in this type of cycles.
16 Although, from the conventional analysis, the exergy destruction rate of boiler is
17 greater than the one of the expander, condenser and pump, the advanced exergy
18 analysis suggests that the first priority of improvement should be given to the
19 expander, followed by the pump, the condenser and the boiler. A total amount of
20 3.75 kW (36.5%) of exergy destruction rate could be lowered, taking account that
21 only the avoidable part of the exergy destruction rate can be reduced.

¹ V. Dolz. CMT-Motores Térmicos, Universitat Politècnica de Valencia, Camino de Vera s/n, 46022 Valencia, Spain.
Phone: +34 963877650 Fax: +34 963877659 e-mail: vidolrui@mot.upv.es

22 **Keywords**

23 Organic Rankine Cycle, Gasoline engine, Waste Heat Recovery, Advanced

24 Exergy analysis

25 **NOMENCLATURE**

26 **Acronyms**

ICE Internal Combustion Engines

ORC Organic Rankine Cycle

WHR Waste Heat Recovery

27 **Notation**

28 **Latin**

\dot{m} Mass flow kg/s

h Specific enthalpy kJ/kg

T Temperature °C

\dot{W} Mechanical power kW

\dot{Q} Thermal power kW

\dot{E} Exergy kW

y Exergy destruction ratio

P Pressure bar

s Specific entropy kJ/kgK

<i>c</i>	Condenser
<i>b</i>	Boiler
<i>p</i>	Pump
<i>cycle</i>	Cycle

32 **Superscripts**

<i>UN</i>	Unavoidable
<i>AV</i>	Avoidable
<i>EN</i>	Endogenous
<i>EX</i>	Exogenous
<i>.</i>	Time rate

33 **1. Introduction**

34 Regulations for ICE-based transportation in the EU seek carbon dioxide
35 emissions lower than 95 g CO₂/km by 2020 [1]. In order to fulfill these limits,
36 improvements in vehicle fuel consumption have to be achieved [2]. One of the
37 main losses of ICEs happens in the exhaust line. Internal combustion engines
38 transform chemical energy into mechanical energy through combustion;
39 however, only about 15-32% of this energy is effectively used to produce work
40 [3], while most of the fuel energy is wasted through exhaust gases and coolant.
41 Therefore, these sources can be exploited to improve the overall efficiency of the
42 engine. Between these sources, exhaust gases show the largest potential of
43 WHR due to its high level of exergy [4], [5]. Regarding WHR technologies,

44 Rankine cycles are considered as the most promising candidates for improving
45 diesel engines [6]. This technology has an impact on the engine performance:

- 46 • Increase of net engine power due to the WHRS
- 47 • Increase of cooling loads comparing to the original engine
- 48 • Increase of total engine weight
- 49 • Increase of pumping losses in the engine

50 According to Battista et al. [7], an overall mean value of 1% fuel consumption
51 reduction can be achieved in light-duty vehicles taking into account the
52 drawbacks of this system.

53 Exergy analysis can identify the sources, magnitude and location of
54 thermodynamic inefficiencies of a system, which can give the appropriate
55 information for improving the overall efficiency of the system focusing in the worse
56 exergy balance elements. The conventional exergy analysis has traditionally
57 been studied and applied to some applications in ICE [8], [9]. However, this
58 analysis is used to evaluate the performance of an individual component, without
59 taking into account interactions among components. Therefore, the advanced
60 exergy analysis [10] was proposed to evaluate energy conversion systems by
61 splitting the exergy in endogenous/exogenous and avoidable/unavoidable.
62 Splitting the exergy into unavoidable and avoidable provides a measure of the
63 potential of improving the efficiency of this component. On the other hand,
64 splitting the exergy into endogenous and exogenous provides information
65 between interactions among system components.

66 This type of analysis has been applied to different energy conversion systems:
67 Kalina cycles in geothermal systems [11], gas turbine systems [12], [13], power

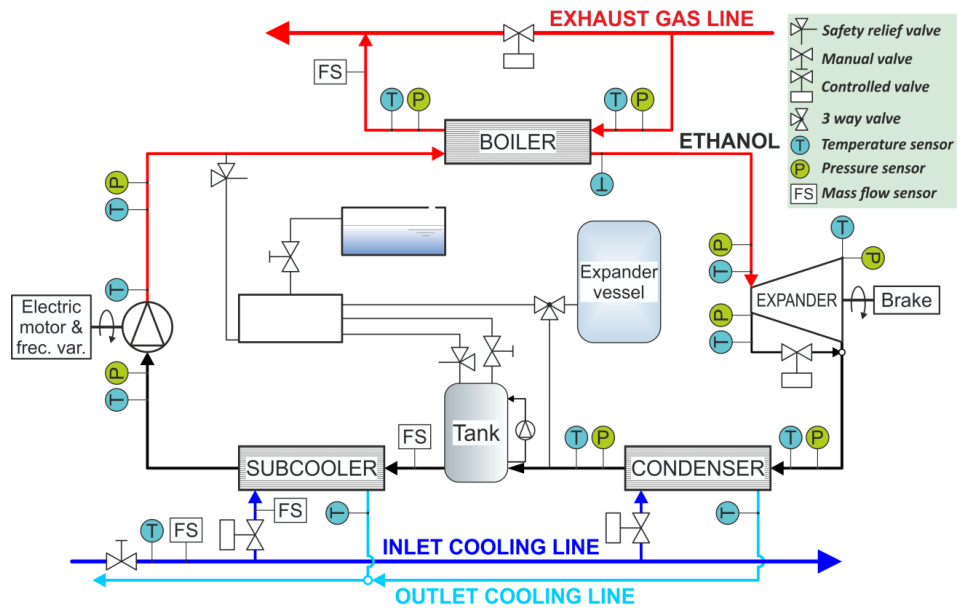
68 plants [14], [15], refrigeration cycles [16], etc.. However, until now no bottoming
69 ORC coupled to an ICE has been analyzed and evaluated using this method.
70 Moreover, values of real experimental tests have been used to this model in order
71 to reproduce actual conditions of these waste heat recovery systems. Hence, on
72 this paper both conventional and advanced exergy analysis were performed to
73 evaluate and analyze a bottoming ORC cycle coupled to an IC engine. The
74 objective of this paper is to quantify, on the basis of reasonable assumptions, the
75 impact of improvements in each component of the system to the global
76 performance of the system using an advanced exergy analysis method [17].

77 The contents of this paper have been ordered in five different sections:

- 78 • Section 1. To introduce the paper.
- 79 • Section 2. To describe and present the experimental setup.
- 80 • Section 3. To explain the conventional and advanced exergy analysis
81 applied to the case of study and the main assumptions.
- 82 • Section 4. To present and analyze the main results of the analysis.
- 83 • Section 5. To understand how the efficiency of the expander and the pinch
84 point affects the cycle performance by means of sensitivity analysis.

85 **2. Description of the ORC**

86 Fig 1 and Fig 2 shows respectively the schematic diagram and the experimental
87 installation of the ORC cycle.



88

89

Fig 1. Schematic diagram of the installation



90

91

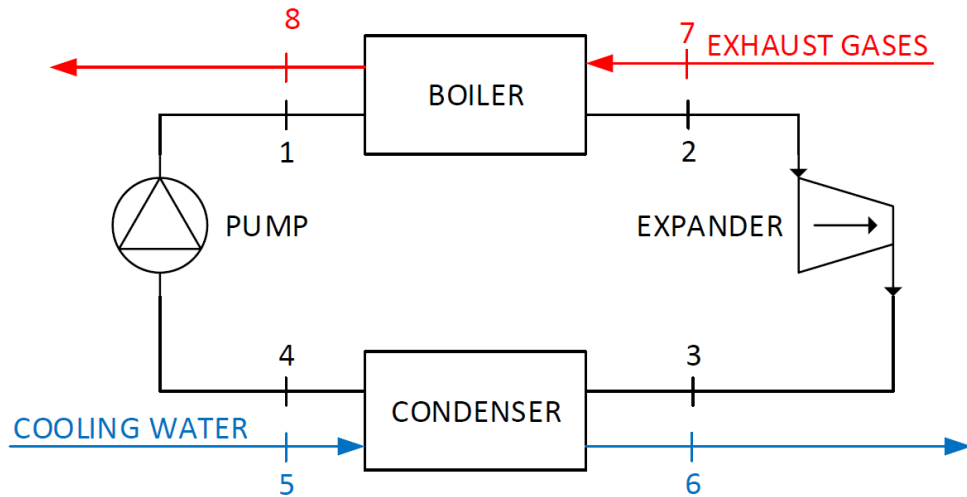
Fig 2. ORC Mock-up

92 The engine exhaust gases provide heat needed to vaporize the ethanol. Among
 93 organic fluids, several authors [18], [19] consider ethanol as a promising fluid due
 94 to its great features in energy recovery aspect in the temperature range of a

95 vehicle application (450 °C - 100 °C). Ethanol has been taken into account for its
96 environmental (low GWP and ODP), thermo-physical properties (high expansion
97 ratios, condensation temperatures at atmospheric pressure and low freezing
98 point) and cost features. The cycle efficiency is higher than other organic fluids
99 such as the R245fa (with higher level of GWP) and new refrigerants such as
100 R1234yf or R1233zd, so the power that can be delivered from the expander
101 considering a machine with the same efficiency will be higher in the case of
102 ethanol cycles. First, the working fluid is pumped from the tank at the condensing
103 pressure to the boiler at the evaporating pressure. Then, the working fluid is pre-
104 heated, vaporized and superheated in the heat exchanger. The ethanol vapor
105 expands from the evaporating pressure to the condensing pressure in the
106 expander machine. Finally, low pressure vapor is extracted from the expander
107 and flows to the condenser, where it condenses using cooling water. The boiler
108 ensures the heat transfer from exhaust gas to the working fluid. The condenser
109 is followed by an expander vessel in order to impose the low pressure in the
110 installation and a liquid reservoir. The expander prototype is a piston swash-plate.

111 **3. Thermodynamic analysis**

112 Fig 3 shows a simplified diagram of the ORC. References to this diagram will be
113 made during the whole article. In this figure, the main elements of the cycle are
114 presented, i.e. boiler, expander, condenser and a pump.



115

116

Fig 3. Cycle diagram for thermodynamic analysis

117

The main assumptions in analyzing the ORC are as follows:

118

- Thermodynamic cycle method [20] was chosen because it is the most convenient method and provides the best results for systems in which a thermodynamic cycle can be defined.

119

120

121

- The system works under steady state conditions.

122

- Energy losses and changes in kinetic and potential energies are neglected [21].

123

124

3.1. Conventional Exergy Analysis

125

The basic equations of the conventional exergy analysis for the K^{th} component of the system (boiler, expander, condenser or pump) are presented in Eq. 1 and 2.

126

127

Using the thermodynamic terms of exergy of fuel and product, the exergy

128

balances for the K^{th} component and for the overall system can be defined.

$$\dot{E}_{F,k} = \dot{E}_{P,k} + \dot{E}_{D,k} \quad (1)$$

$$\dot{E}_{F,tot} = \dot{E}_{P,tot} + \dot{E}_{L,tot} + \dot{E}_{D,tot} \quad (2)$$

$$\varepsilon_k = \frac{\dot{E}_{P,k}}{\dot{E}_{F,k}} = 1 - \frac{\dot{E}_{D,k}}{\dot{E}_{F,k}} \quad (3)$$

$$y_{D,k} = \frac{\dot{E}_{D,k}}{\dot{E}_{F,k}} \quad (4)$$

$$y_{D,k}^* = \frac{\dot{E}_{D,k}}{\dot{E}_{D,tot}} \quad (5)$$

129 Where $\dot{E}_{F,k}$, $\dot{E}_{P,k}$ and $\dot{E}_{D,k}$ are respectively the exergy rate of fuel, product and
 130 internal exergy loss in the Kth component. The subscript *tot* means the total
 131 amount of the overall system. $\dot{E}_{L,tot}$ corresponds to external exergy loss in the
 132 overall system. ε_k , $y_{D,k}$ and $y_{D,k}^*$ are the exergy efficiency, the exergy destruction
 133 ratio and the exergy rate of fuel with the total exergy destruction respectively.

134 The exergy destruction (or internal exergy loss) is the exergy destroyed due to
 135 irreversibility within a system or a Kth component. At the component level, exergy
 136 flows are associated with fuel or product in each component. Therefore, the
 137 exergy loss in the Kth component is related with the transfer of thermal energy to
 138 the ambient (heat loss). The exergy loss (or external exergy loss) is the exergy
 139 transfer from the system to the surroundings. Considering the boundaries of the
 140 component analysis fixed at ambient temperature, the exergy loss is 0 and the
 141 thermodynamic inefficiencies consist only of exergy destruction. Therefore, the
 142 exergy loss is related only with the overall system and not with the Kth component.

143 The energy and exergy balances for the system components as control volumes
 144 are presented in Table 1 and Table 2.

Table 1. Energy balance equations

Cycle component	Energy balance equations
Expander	$\eta_{exp} = \frac{\dot{W}_{exp}}{\dot{W}_{exp,iso}}, \dot{W}_{exp,iso} = \dot{m}_{et} * (h_2 - h_{3,iso}), \dot{W}_{exp} = \dot{m}_{et} * (h_2 - h_3)$
Pump	$\eta_p = \frac{\dot{W}_{p,iso}}{\dot{W}_p}, \dot{W}_{p,iso} = \dot{m}_{et} * (h_{1,iso} - h_4), \dot{W}_p = \dot{m}_{et} * (h_1 - h_4)$
Condenser	$\dot{Q}_c = \dot{m}_{et} * (h_3 - h_4)$
Boiler	$\dot{Q}_e = \dot{m}_{et} * (h_2 - h_1)$

146

147

Table 2. Exergy balance equations

Cycle component	Exergy balance equations
Expander	$\dot{E}_2 = \dot{E}_3 + \dot{W}_{exp} + \dot{E}_{D,exp}$
Pump	$\dot{E}_4 + \dot{W}_p = \dot{E}_1 + \dot{E}_{D,p}$
Condenser	$\dot{E}_3 + \dot{E}_5 = \dot{E}_4 + \dot{E}_6 + \dot{E}_{D,c}$
Boiler	$\dot{E}_7 + \dot{E}_1 = \dot{E}_2 + \dot{E}_8 + \dot{E}_{D,b}$

148

149 3.2. Advanced Exergy Analysis

150 In the advanced exergy analysis [17], the rate of exergy destruction in the Kth
 151 component of the system is split into endogenous / exogenous and avoidable /
 152 unavoidable.

153 *Endogenous/Exogenous*

154 Endogenous exergy destruction in K^{th} component is related to the irreversibility
155 occurring inside this component, whereas the exogenous part is associated with
156 the irreversibilities taking place in the rest of the components of the system [17].
157 Therefore, the endogenous exergy destruction in K^{th} component ($\dot{E}_{D,k}^{EN}$) is the part
158 of the total exergy destruction in the K^{th} component ($\dot{E}_{D,k}$) obtained considering
159 that all the components operate ideally and the component being examined
160 operates with real efficiency (Hybrid Process). In a Hybrid Process (or Hybrid
161 Cycle) only one component is real, i.e., operates with its real efficiency, while all
162 other components operate in a theoretical way. In this case, the exergy
163 destruction within the component being considered represents the endogenous
164 exergy destruction. Thus, step-by-step introducing irreversibilities successively in
165 each system component the endogenous exergy destruction within each
166 component is calculated. Therefore, in order to compute the endogenous exergy
167 destruction in the K^{th} component ($\dot{E}_{D,k}^{EN}$), a Hybrid Cycle for each component has
168 to be simulated. Exogenous exergy destruction ($\dot{E}_{D,k}^{EX}$) is the difference between
169 the exergy destruction value of the variable within the component in the real
170 system ($\dot{E}_{D,k}$) and the endogenous part ($\dot{E}_{D,k}^{EN}$). Eq. 1 shows the splitting between
171 both parts, where EN and EX indicate the endogenous and exogenous parts,
172 respectively.

$$\dot{E}_{D,k} = \dot{E}_{D,k}^{EN} + \dot{E}_{D,k}^{EX} \quad (1)$$

173 Moreover, the exogenous exergy destruction can be further split (Eq. 2) as the
174 effect of exergy destruction within the r^{th} component caused by the exergy
175 destruction of the K^{th} component and a term called exogenous exergy

176 destruction ($\dot{E}_{D,k}^{MX}$) [15], which considers the simultaneous interactions of all other
177 n-1 elements.

$$\dot{E}_{D,k}^{EX} = \dot{E}_{D,k}^{MX} + \sum_{\substack{r=1 \\ r \neq k}}^n \dot{E}_{D,k}^{EX,r} \quad (2)$$

178 *Avoidable/Unavoidable*

179 Unavoidable exergy destruction in K^{th} component cannot be reduced due to
180 technological limitations (material characteristics, production costs and
181 manufacturing methods), whereas the avoidable part, which is the remaining part,
182 can be reduced improving the design of this component [17]. Therefore, the
183 unavoidable exergy destruction ($\dot{E}_{D,k}^{UN}$) is the part of total exergy destruction within
184 the K^{th} component ($\dot{E}_{D,k}$) considering that all the components operate in
185 unavoidable conditions. Avoidable exergy destruction ($\dot{E}_{D,k}^{AV}$) in the K^{th} component
186 is the difference between the exergy destruction value of the variable within the
187 K^{th} component in the real system ($\dot{E}_{D,k}$) and the unavoidable part ($\dot{E}_{D,k}^{UN}$). Eq. 3
188 shows the splitting between both parts, where UN and AV indicate the
189 unavoidable and avoidable parts, respectively.

$$\dot{E}_{D,k} = \dot{E}_{D,k}^{UN} + \dot{E}_{D,k}^{AV} \quad (3)$$

190 In order to obtain the unavoidable exergy destruction Eq. 4 was proposed by
191 Tsatsaronis et. al [22]. In order to obtain the ratio $\left(\frac{\dot{E}_D}{\dot{E}_P}\right)_k^{UN}$ for the K^{th} component,
192 the system is solved considering that each component operates under the best
193 possible conditions considering technological limitations. This ratio is the main
194 parameter to calculate the unavoidable part of the exergy destruction rate of each
195 individual component in a real process.

$$\dot{E}_{D,k}^{UN} = \dot{E}_{P,k} * \left(\frac{\dot{E}_D}{\dot{E}_P} \right)_k^{UN} \quad (4)$$

196

197 3.2.1 Combination of the splitting

198 By combining the two splitting approaches, the unavoidable-exogenous
 199 $(\dot{E}_{D,k}^{UN,EX})$, the unavoidable-endogenous $(\dot{E}_{D,k}^{UN,EN})$, the avoidable-exogenous
 200 $(\dot{E}_{D,k}^{AV,EX})$ and the avoidable-endogenous $(\dot{E}_{D,k}^{AV,EN})$ values can be obtained using
 201 Eq. 5, 6, 7 and 8.

$$\dot{E}_{D,k}^{UN,EN} = \dot{E}_{P,k}^{EN} * \left(\frac{\dot{E}_D}{\dot{E}_P} \right)_k^{UN} \quad (5)$$

$$\dot{E}_{D,k}^{UN,EX} = \dot{E}_{D,k}^{UN} - \dot{E}_{D,k}^{UN,EN} \quad (6)$$

$$\dot{E}_{D,k}^{AV,EN} = \dot{E}_{D,k}^{EN} - \dot{E}_{D,k}^{UN,EN} \quad (7)$$

$$\dot{E}_{D,k}^{AV,EX} = \dot{E}_{D,k}^{EX} - \dot{E}_{D,k}^{UN,EN} \quad (8)$$

202 3.3. Assumptions

203 In this analysis, three thermodynamic cycles were proposed, i.e. real, ideal and
 204 unavoidable. The following assumptions were adopted:

- 205 • In the real cycle, isentropic efficiencies of the expander machine and
 206 the pump, pinch point and pressure drops in the heat exchangers are
 207 obtained by experimental points presented in previous articles [23].

- 208 • In the ideal cycle, isentropic efficiencies of expander and pump and
 209 efficiencies of condenser and boiler are considered 100%. Pressure
 210 drops are assumed to be zero on condenser and boiler processes.
- 211 • In the unavoidable cycle, efficiencies of the expander and the pump
 212 are considered respectively 80% [24] and 95% [25], assuming this level
 213 the maximum that could be exceeded due to technological limitations.
 214 Improvements in valve timing and oil refrigeration loop should be
 215 made. Pinch points and pressure drops in this cycle are lower than the
 216 real cycle but also considering technological limitations [26].

217 Table 3 shows a summary of these variables used to define the different
 218 cycles.

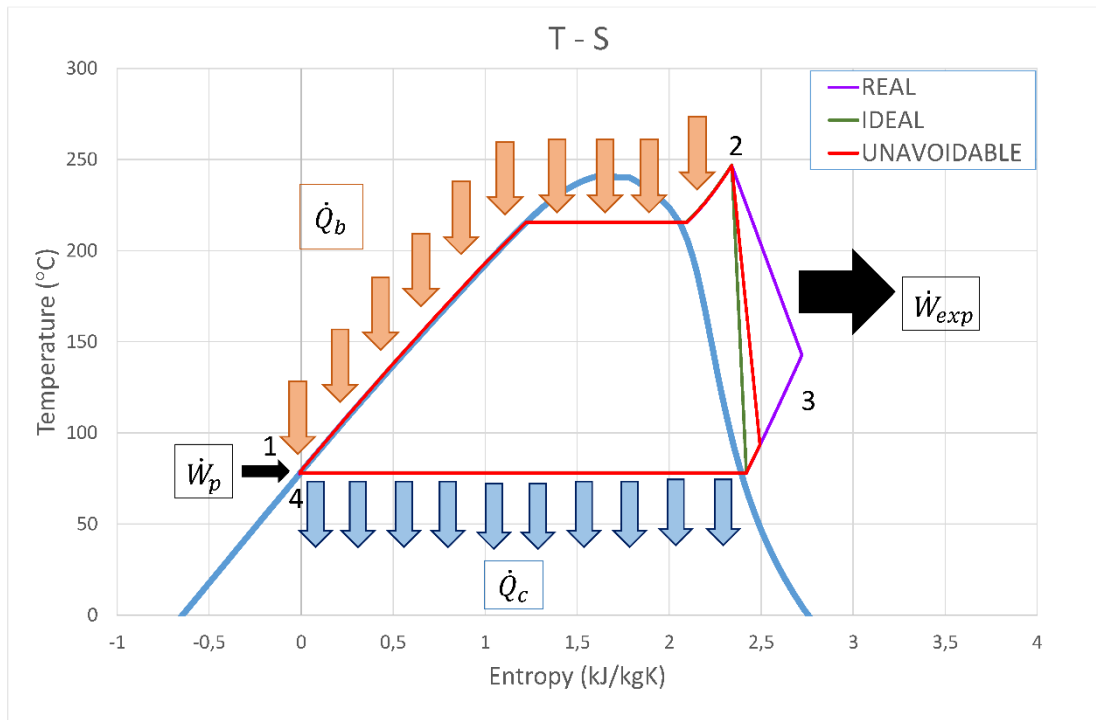
219 *Table 3. Assumptions for real, ideal and unavoidable*

Component		Real		Ideal		Unavoidable
Expander	η_{exp}	43%	η_{exp}	100%	η_{exp}	80%
	$\Delta T_{pp} (^{\circ}C)$	5.00	$\Delta T_{pp} (^{\circ}C)$	0	$\Delta T_{pp} (^{\circ}C)$	2
Condenser	ΔP	1.60%	ΔP	0%	ΔP	1%
	εC	83%	εC	100%	εC	90%
Pump	η_p	89%	η_p	100%	η_p	95%
	$\Delta T_{pp} (^{\circ}C)$	50.00	$\Delta T_{pp} (^{\circ}C)$	0	$\Delta T_{pp} (^{\circ}C)$	10
Boiler	ΔP	0.79%	ΔP	0%	ΔP	0.5%
	εb	98%	εb	100%	εb	99.0%

220 4. Simulation results and discussion

221 For the exergy analysis, steady-state simulations were performed by modeling
 222 the cycle described on Fig 3. As shown in Fig 4, the evaporation process
 223 corresponds to 1-2, the expansion process to 2-3, the condensation process to
 224 3-4 and the pumping process to 4-1. The major difference between these cycles
 225 correspond to the expansion process (2-3). In order to optimize the cycle, get the
 226 maximum power in the expander and avoid entering the two-phase zone during

227 expansion, the high pressure has been set to $0.65 \cdot P_{critical}$ and the low pressure to
 228 1 bar to avoid air intakes in the ducts. Depending on the cycle, different pressure
 229 drops have been taken into account.
 230



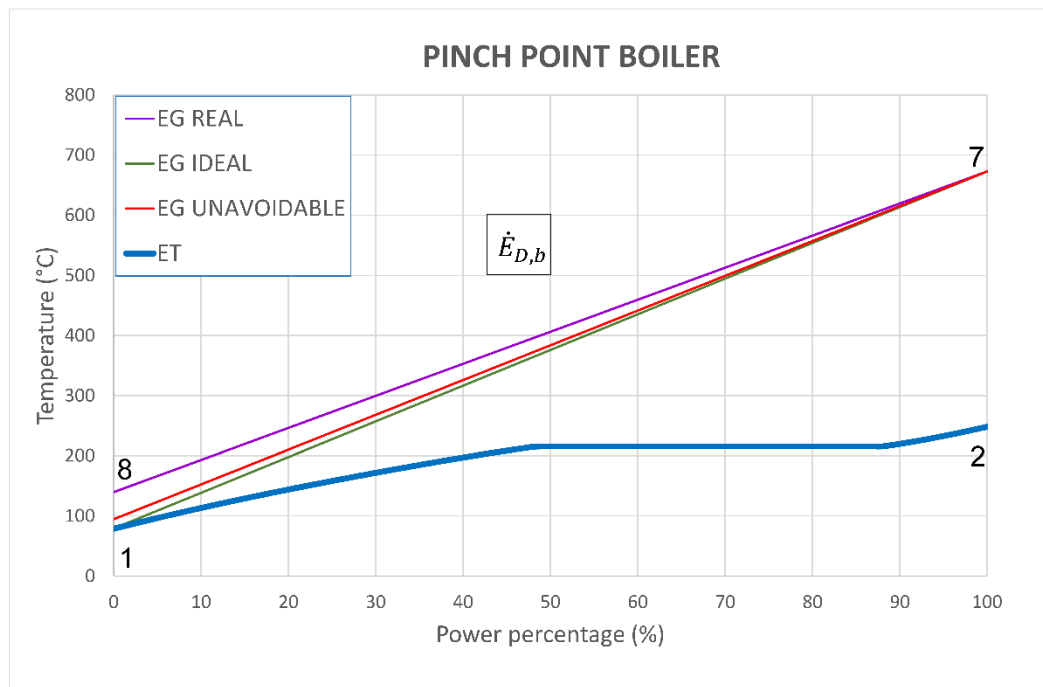
231

232

Fig 4. Ideal, real and unavoidable cycles in the T-S Diagram

233 Fig 5 shows the evaporation process in the three cycles: ideal, real and
 234 unavoidable. In all these cycles, the inlet temperature and the mass flow of
 235 exhaust gases have remained constant. Depending on the cycle, the pinch point
 236 changes from 50 °C in the real case, 10 °C in the unavoidable case and 0 °C in
 237 the ideal one. A change of temperature at the outlet of exhaust gases implies a
 238 change in the power released by the boiler and thus, the ethanol mass flow
 239 flowing in the cycle. Therefore, in order to visualize the evaporation process in
 240 the three cycles, the power percentage in % have been plotted in the X axis. The
 241 exergy destruction in the boiler is proportional to the area between exhaust gases

242 and ethanol. As it can be seen in this figure, the exergy destruction in the ideal
243 case is lower than the real one.



244

245 *Fig 5. Ideal, real and unavoidable cycles in the evaporation process*

246 Table 4, Table 5 and Table 6 indicate the thermodynamic properties and the mass
247 flow rates at different state points of the ORC (Fig 3) under real, ideal and
248 unavoidable conditions respectively. As previously mentioned, the ethanol mass
249 flow in the cycle is higher in the ideal case than in the real one due to
250 thermodynamic restrictions. Pressure drop in the boiler and the condenser have
251 been considered both in the real and unavoidable case. The last two columns are
252 related with the calculation of exergy in each state point.

253

254

255

256

Table 4. Thermodynamic properties and mass flow rates of the ORC under real conditions

Point	T (°C)	P (bar)	h (kJ/kg)	\dot{m} (kg/s)	s (kJ/kgK)	e (kJ/kg)	\dot{E} (kW)
1	78.54	39.65	262.8	0.02623	1.028	17.49	0.459
2	246.6	39.65	1336	0.02623	3.39	386.8	10.146
3	142.7	0.984	1229	0.02623	3.768	166.7	4.373
4	77.53	0.984	256.9	0.02623	1.026	12.16	0.319
5	50	1.5	209.4	0.2083	0.7037	4.252	0.886
6	74.88	1.5	313.5	0.2083	1.014	15.87	3.306
7	672.8	1.071	985	0.04799	6.888	331	15.885
8	128.5	1.013	403	0.04799	5.996	14.86	0.713

257

258

Table 5. Thermodynamic properties and mass flow rates of the ORC under ideal conditions

Point	T (°C)	P (bar)	h (kJ/kg)	\dot{m} (kg/s)	s (kJ/kgK)	e (kJ/kg)	\dot{E} (kW)
1	78.7400	39.96	263.5	0.02923	1.029	17.63	0.515
2	247	39.96	1336	0.02923	3.39	387.2	11.318
3	78.5	1	1087	0.02923	3.39	137.6	4.022
4	77.94	1	258.2	0.02923	1.029	12.35	0.361
5	50	1.5	209.4	0.2083	0.7037	4.252	0.886
6	77.81	1.5	325.8	0.2083	1.049	17.68	3.683
7	672.8	1.071	985	0.04799	6.888	331	15.885
8	78.74	1.013	352.7	0.04799	5.862	4.346	0.209

259

260

Table 6. Thermodynamic properties and mass flow rates of the ORC under unavoidable conditions

Point	T (°C)	P (bar)	h (kJ/kg)	\dot{m} (kg/s)	s (kJ/kgK)	e (kJ/kg)	\dot{E} (kW)
1	78.58	39.76	262.9	0.02845	1.028	17.52	0.498
2	246.7	39.76	1336	0.02845	3.39	386.9	11.007
3	93.45	0.99	1136	0.02845	3.531	145	4.125
4	77.68	0.99	257.4	0.02845	1.027	12.23	0.348
5	50	1.5	209.4	0.2083	0.7037	4.252	0.886
6	75.84	1.5	317.6	0.2083	1.026	16.45	3.427
7	672.8	1.071	985	0.04799	6.888	331	15.885
8	88.58	1.013	362.6	0.04799	5.89	5.984	0.287

261

262 Table 7 shows the net power and the cycle energy efficiency and cycle exergy
 263 efficiency for ideal, unavoidable and real cases. As it can be seen, net power is
 264 reduced in the real cycle because two effects: lower ethanol mass flow due to
 265 higher pinch point in the boiler and lower isentropic efficiency in the expander. As

266 a global consequence, both the cycle energy efficiency (defined as the net power
 267 divided by the power of the boiler) and cycle exergy efficiency (defined as the net
 268 power divided by the exergy rate of fuel in the boiler) are reduced comparing them
 269 to the ideal cycle. Therefore, cycle efficiency corresponds to 22.72% in the ideal
 270 case and technical limitations give a value of 18.13% in the case of unavoidable
 271 cycle. The real cycle gives a value of 9.42%. These values correspond to the
 272 ones found in literature [27].

273

Table 7. Power and efficiency of ideal, unavoidable and real cycles

	Ideal	Unavoidable	Real
\dot{W}_{exp} (kW)	7.28	5.69	2.81
\dot{W}_p (kW)	0.15	0.16	0.15
\dot{W}_{net} (kW)	7.12	5.53	2.65
\dot{Q}_b (kW)	31.35	30.53	28.15
\dot{Q}_c (kW)	24.23	25.00	25.50
\dot{E}_b (kW)	15.67	15.59	15.17
η_{cycle}	22.72%	18.13%	9.42%
ε_{cycle}	45.44%	35.48%	17.48%

274

275 Considering conventional exergy equations applied to this particular application
 276 and presented in Table 2, the following results are obtained. The total exergy fuel
 277 rate is the difference between exergy rates of exhaust gases entering and ethanol
 278 leaving the boiler. The expander power output is considered the rate of total
 279 products exergy. Table 8, Table 9 and Table 10 show the results of conventional
 280 exergy analysis for ORC under real, ideal and unavoidable conditions
 281 respectively.

282

283

284

Table 8. Results of conventional exergy analysis under real conditions

Component	E_F (kW)	E_P (kW)	E_D (kW)	ϵ	Y_k	Y_k^*
Expander	5.77	2.81	2.97	49%	51%	29%
Pump	0.33	0.14	0.19	42%	58%	2%
Condenser	4.05	2.42	1.63	60%	40%	16%
Boiler	15.17	9.69	5.48	64%	36%	53%
Overall System	15.17	2.81	10.84	18%	71%	100%

285

286

Table 9. Results of conventional exergy analysis under ideal conditions

Component	E_F (kW)	E_P (kW)	E_D (kW)	ϵ	Y_k	Y_k^*
Expander	7.30	7.28	0.02	99.8%	0.2%	0.3%
Pump	0.15	0.15	0.00	99.6%	0.4%	0.0%
Condenser	3.66	2.80	0.86	76.4%	23.6%	15.0%
Boiler	15.68	10.80	4.87	68.9%	31.1%	84.7%
Overall System	15.68	7.28	5.76	46.4%	36.7%	100.0%

287

288

Table 10. Results of conventional exergy analysis under unavoidable conditions

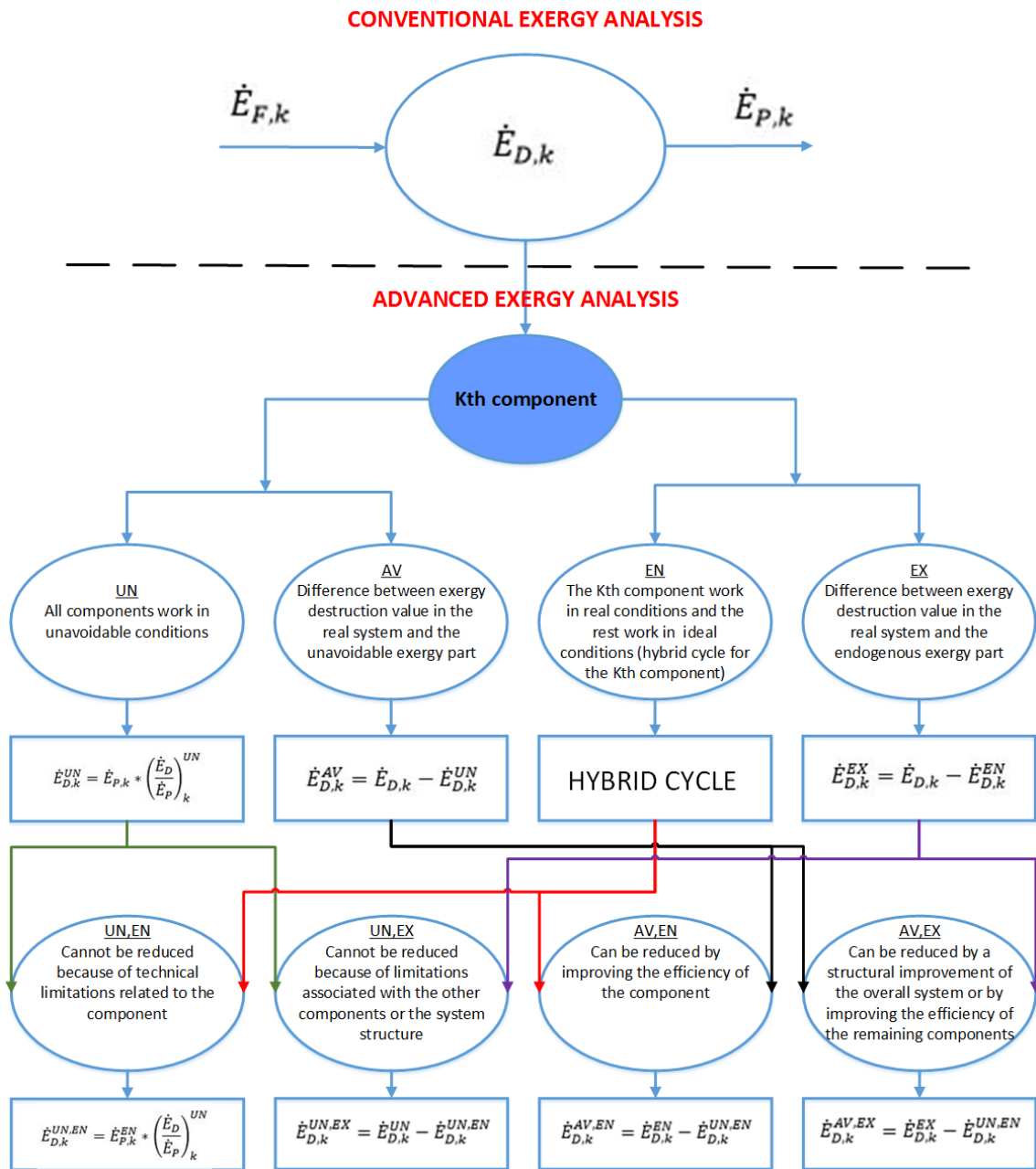
Component	E_F (kW)	E_P (kW)	E_D (kW)	ϵ	Y_k	Y_k^*
Expander	6.88	5.69	1.19	83%	17%	16%
Pump	0.22	0.15	0.07	67%	33%	1%
Condenser	3.78	2.54	1.24	67%	33%	16%
Boiler	15.60	10.51	5.09	67%	33%	67%
Overall System	15.60	5.69	7.59	36%	49%	100%

289

290 Based on the results obtained from conventional analysis (Table 8), the overall
 291 system should be improved following priorities for the components with higher
 292 exergy destruction: boiler (5.48 kW), expander (2.97 kW), condenser (1.63 kW)
 293 and pump (0.19 kW). In order to increase the ORC efficiency a reduction in
 294 exergy destruction rates are needed. From a conventional exergy analysis, it is
 295 not possible to distinguish between irreversibilities occurring in other components
 296 and the component itself. The advanced exergy analysis [28] evaluates the
 297 detailed interactions between components of the overall system, and the real
 298 potential of improvement a component within a system.

299 In the advanced exergy analysis the endogenous exergy destruction rate for the
300 K^{th} component is obtained by calculating several cycles (the same as number of
301 components) considering the component under study with real values of the
302 parameter and the rest with ideal conditions. The exogenous exergy destruction
303 rate will be calculated by difference to the total exergy destruction (Eq. 1). The
304 unavoidable exergy destruction rate is obtained when all the components work
305 under unavoidable conditions. Once the unavoidable conditions are calculated,
306 the ratio of exergy destruction to the product exergy rate is computed (Eq. 4). The
307 avoidable exergy destruction rate will be computed by difference (Eq. 3). To split
308 the exergy between unavoidable-exogenous, unavoidable-endogenous,
309 avoidable-exogenous and avoidable-endogenous Eq. 5 to 8 were applied.

310 Fig 6 shows a flow chart of exergy destruction rate in the K^{th} component.



311

312

Fig 6. Flow chart of exergy destruction rate (Conventional and Advanced) in the K^{th} component

313

314

Results from the previous analysis are presented in Table 11.

315

316

317

Table 11. Results of advanced exergy analysis (kW)

Component	\dot{E}_D	\dot{E}_D^{EN}	\dot{E}_D^{EX}	\dot{E}_D^{AV}	\dot{E}_D^{UN}	$\dot{E}_D^{AV,EN}$	$\dot{E}_D^{UN,EN}$	$\dot{E}_D^{AV,EX}$	$\dot{E}_D^{UN,EX}$
Boiler	5.48	5.48	0.00	0.79	4.69	0.79	4.69	0.00	0.00
Expander	2.97	3.29	-0.32	2.38	0.59	2.63	0.66	-0.25	-0.07
Condenser	1.63	1.37	0.26	0.46	1.18	0.27	1.10	0.19	0.08
Pump	0.19	0.21	-0.02	0.12	0.07	0.13	0.08	-0.01	-0.01
Overall System	10.27	10.35	-0.07	3.75	6.52	3.82	6.53	-0.07	0.00

319

320 As shown in Table 11, the value of endogenous exergy is greater than the value
 321 of exogenous exergy in all the system components. Therefore, the greatest
 322 contribution to the exergy destruction rate in each of the components comes from
 323 the internal irreversibility of the component itself. Regarding to exogenous
 324 exergy, the condenser have the highest value (0.26 kW). Therefore, a
 325 modification in the other component efficiencies can lead to a reduction in the
 326 exergy destruction rate of this element and an improvement in overall cycle
 327 efficiency.

328 Interactions between different components can be positive or negative. These
 329 two impacts could be the result of mass flow changes or thermodynamic property
 330 variation of material flows through the K^{th} component due to the introduction of
 331 additional irreversibilities in the system. In this system, some components have
 332 values of endogenous exergy greater than the exergy destruction rate itself. This
 333 can be analyzed by the results of the specific advanced exergy analysis (Table
 334 12). Table 12 shows that the system is more efficient (less exergy destroyed in
 335 kJ/kg for all the components) in the endogenous case than in the real case.
 336 However, changing the conditions from the ideal case to the endogenous case
 337 (the K^{th} component is real and the rest are ideal), the ethanol mass flow changes
 338 between both cases due to changes in the pinch point. Hence, the result is that

339 the endogenous exergy destruction rate in kW is higher than the real exergy
 340 destruction rate in the expander and pump (Table 11).

341 *Table 12. Results of specific advanced exergy analysis (kJ/kg)*

Component	E_D	E_D^{EN}	E_D^{EX}	E_D^{AV}	E_D^{UN}	$E_D^{AV,EN}$	$E_D^{UN,EN}$	$E_D^{AV,EX}$	$E_D^{UN,EX}$
Expander	113.10	112.50	0.60	90.68	22.42	90.08	22.42	0.60	0.00
Pump	7.22	7.17	0.05	4.64	2.59	4.56	2.61	0.07	-0.02
Condenser	62.28	46.84	15.44	17.38	44.90	9.11	37.72	8.27	7.17
Evaporator	209.09	187.51	21.59	30.27	178.83	27.01	160.50	3.26	18.33
Overall System	391.70	354.02	37.68	142.97	248.73	130.77	223.25	12.20	25.48

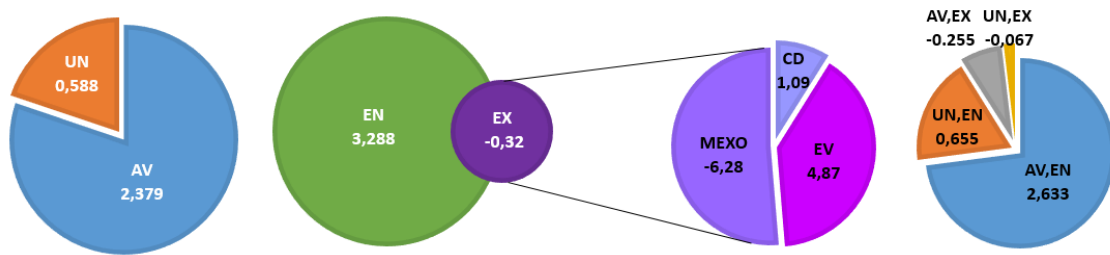
342

343 Another important point observed from Table 11 is that a total amount of 3.75 kW
 344 could be lowered; taking into account that only the avoidable part of the exergy
 345 destruction rate can be reduced. This part of the exergy is higher than the
 346 unavoidable part in the expander (2.38 kW vs 0.59 kW) and the pump (0.12 vs
 347 0.07 kW). These components will have the highest improvement potential by
 348 technical modifications of the components.

349 As the avoidable-endogenous part corresponds to the part of the exergy
 350 destruction rate, which can be reduced by increasing the efficient of the
 351 component, it will be the main focus. The avoidable-endogenous rate is higher
 352 than the unavoidable-endogenous rate in the expander and the pump. As stated
 353 before, technical modifications of these components will improve efficiency of the
 354 ORC system. Regarding the avoidable-exogenous rate, it is higher than the
 355 exogenous-unavoidable rate in the condenser. Therefore, an improvement in the
 356 efficiency of other components plays an important role in enhancing the efficiency
 357 of the condenser. The avoidable-endogenous part of the exergy destruction is
 358 higher than the avoidable-exogenous part in all the components. This difference

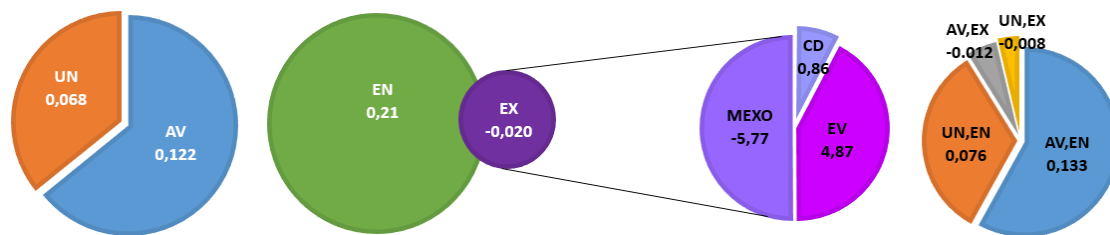
359 is much higher in the expander, thus an optimization in this component will be
 360 essential to improve global ORC performance.

361 Results of splitting exergy destruction rate of the components are shown in Fig 7,
 362 Fig 8, Fig 9 and Fig 10. As a global consequence under the working conditions
 363 for the present work, there is a high potential of improvement in the ORC system,
 364 focusing in the expander. From the total exergy destruction rate in the expander
 365 (2.97 kW), the greater part of the exergy (88%) can be reduced by technological
 366 improvement of the component itself (avoidable-endogenous). In the pump,
 367 condenser and boiler this potential is reduced to 70%, 16% and 14% respectively.



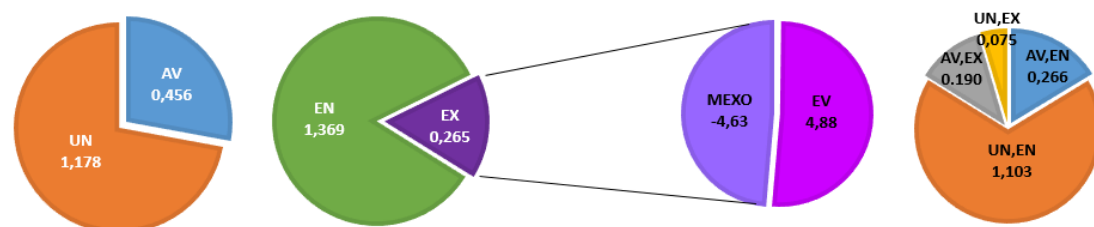
368

369 *Fig 7. Results of splitting the exergy destruction rate for the expander*



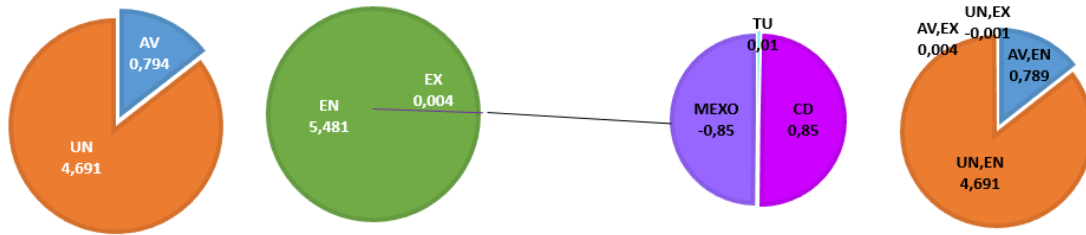
370

371 *Fig 8. Results of splitting the exergy destruction rate for the pump*



372

373 *Fig 9. Results of splitting the exergy destruction rate for the condenser*



374

375

Fig 10. Results of splitting the exergy destruction rate for the boiler

376

5. Sensitivity analysis

377

The expander efficiency and the pinch point are the critical parameters of this

378

cycle, therefore, a sensibility analysis varying both parameters is presented.

379

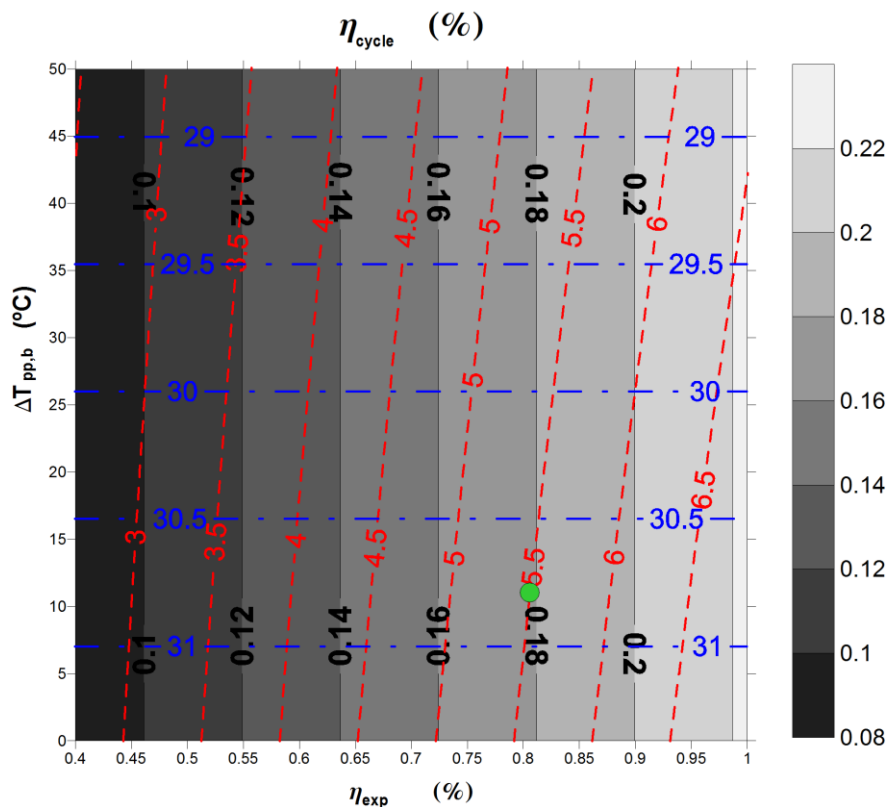
Cycle efficiency as a function of both parameters is plotted in Fig 11. Moreover,

380

blue lines correspond to boiler exchanged power and red ones to expander power

381

in kW. The green point correspond to the unavoidable conditions.



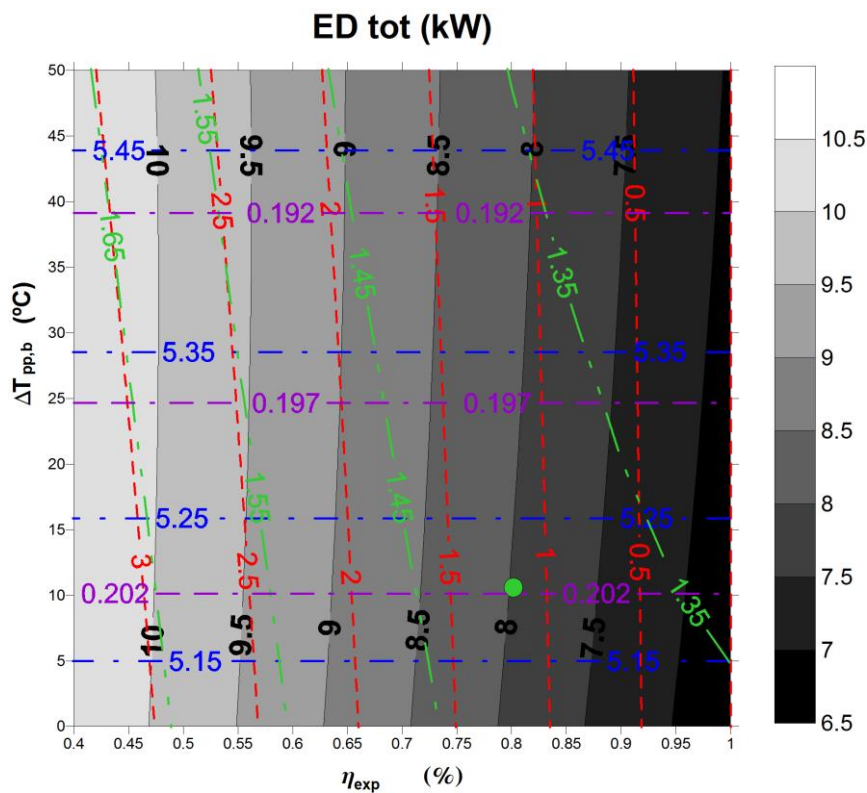
382

383
384

Fig 11. Cycle efficiency, boiler exchanged power (blue lines, kW) and expander power (red lines, kW) as a function of the pinch point and expander efficiency

385 As it is shown, the pinch point has a direct influence in the boiler power. The boiler
 386 power decrease with higher pinch points because the temperature difference in
 387 the boiler decreases. Regarding the expander power, it increases with higher
 388 expander efficiencies and lower pinch points. The former has an influence in the
 389 enthalpy drop in the expansion process and the latter on the ethanol mass flow
 390 in the cycle. The relation between both values give the cycle energy efficiency. A
 391 maximum value of 21% can be obtained in the best conditions of the cycle.

392 In order to discriminate the contributions of each component to the global exergy
 393 destruction rate, Fig 12 is presented. Blue lines correspond to the boiler, red ones
 394 to the expander, green ones to the condenser and pink ones to the exergy
 395 destruction rate of pump in kW. The sum of all components exergy destruction
 396 rate is plotted as a contour map behind them.



397

398 Fig 12. Contribution of boiler (blue lines, kW), expander (red lines, kW), condenser (green lines, kW) and
 399 pump (purple lines, kW) to the global exergy destruction rate (kW) as a function of the pinch point and
 400 expander efficiency.

401 As it can be shown in Fig 12, exergy destruction rate in the boiler and the pump
402 depends on the pinch point. The former increases with pinch point and the latter
403 decreases with it. Boiler exergy destruction rate increases because the area
404 between ethanol evaporation process and the exhaust gases process increases
405 too (Fig 5). As the temperature difference decrease with higher pinch points, the
406 boiler power released to the cycle is lower and thus, the ethanol mass flow too.
407 This is the reason why the exergy destruction in the pump decreases with the
408 pinch point and remain approximately constant with expander efficiency. As
409 stated before, increasing the expander efficiency will reduce the exergy
410 destruction rate in the expander. The relation with the condenser depends on
411 both parameters, the pinch point (and thus, the ethanol mass flow) and the
412 expander efficiency. To sum up, reducing the pinch point in the boiler and
413 increasing the expander efficiency will reduce the exergy destruction rate from
414 10.5 kW to 6.5 kW.

415 **6. Conclusions**

416 This paper evaluates and analyzes a bottoming ORC cycle coupled to an IC
417 engine by means of conventional and advanced exergy analysis. The following
418 results have been obtained:

- 419 1. Conventional analysis shows that the overall system should be improved
420 following priorities for the components in this order: boiler, expander,
421 condenser and pump. However, the advanced exergy analysis suggests
422 that the first priority should be given to the expander, followed by the pump,
423 condenser and boiler.

424 2. The value of endogenous exergy is greater than the value of exogenous
425 exergy in all the system components. Therefore, the greatest contribution
426 to the exergy destruction rate in each of the components comes from the
427 internal irreversibility of the component itself and a minimum exergy
428 destruction comes from other components as external irreversibility.
429 Regarding to exogenous (external irreversibilities) exergy destruction, the
430 condenser has the highest value (0.26 kW, 16% of the total exergy
431 destruction rate). Therefore, a modification in the other component
432 efficiencies can lead to a reduction in the exergy destruction rate of this
433 component and an improvement in cycle efficiency.

434 3. A total amount of 3.75 kW, 36.5% of exergy destruction rate, could be
435 lowered, taking account that only the avoidable part (considering an
436 estimation of maximum efficiencies on the cycle components) of the
437 exergy destruction rate can be reduced. This part of the exergy is higher
438 than the unavoidable part in the expander (2.38 kW vs 0.59 kW) and the
439 pump (0.12 vs 0.07 kW). These two components will have the highest
440 improvement potential by technical modifications of the components.

441 4. Considering the sensibility analysis varying the pinch point from 0°C to
442 50°C in the boiler and the expander efficiency from 0.4 to 1 under the
443 working conditions of the study, a maximum cycle efficiency of 21% can
444 be obtained in comparison with 10% in the real conditions. Regarding the
445 overall exergy destruction rate of the cycle, it could be lowered from 10.5
446 kW to 6.5 kW.

447 7. Acknowledgements

448 This work is part of a research project called “Evaluation of bottoming cycles in
449 IC engines to recover waste heat energies” funded by a National Project of the
450 Spanish Government with reference TRA2013-46408-R. Authors want to
451 acknowledge the “Apoyo para la investigación y Desarrollo (PAID)” grant for
452 doctoral studies (FPI S2 2015 1067).

453 REFERENCES

-
- 454 [1] L. Arnaud, G. Ludovic, D. Mouad, Z. Hamid, and L. Vincent, “Comparison
455 and Impact of Waste Heat Recovery Technologies on Passenger Car Fuel
456 Consumption in a Normalized Driving Cycle,” *Energies*, vol. 7, no. 8, pp.
457 5273–5290, 2014.
- 458 [2] F. Payri, J. Luján, C. Guardiola, and B. Pla, “A Challenging Future for the
459 IC Engine: New Technologies and the Control Role,” *Oil Gas Sci. Technol.*
460 – *Rev. d’IFP Energies Nouv.*, vol. 70, pp. 15–30, 2014.
- 461 [3] R. El Chammas, D. Clodic, and R. El Chammas, “Combined Cycle for
462 Hybrid Vehicles,” *SAE Int.*, vol. 1, no. 724, pp. 1–10, Apr. 2005.
- 463 [4] V. Macián, J. R. Serrano, V. Dolz, and J. Sánchez, “Methodology to design
464 a bottoming Rankine cycle, as a waste energy recovering system in
465 vehicles. Study in a HDD engine,” *Appl. Energy*, vol. 104, pp. 758–771,
466 Apr. 2013.
- 467 [5] H. Teng, G. Regner, and C. Cowland, “Waste Heat Recovery of Heavy-
468 Duty Diesel Engines by Organic Rankine Cycle Part I: Hybrid Energy
469 System of Diesel and Rankine Engines,” *SAE Int.*, vol. 1, no. 724, pp. 1–
470 13, Apr. 2007.
- 471 [6] S. N. Hossain and S. Bari, “Waste heat recovery from the exhaust of a
472 diesel generator using Rankine Cycle,” *Energy Convers. Manag.*, vol. 75,
473 pp. 141–151, 2013.
- 474 [7] D. Di Battista, M. Mauriello, and R. Cipollone, “Effects of an ORC Based
475 Heat Recovery System on the Performances of a Diesel Engine,” *SAE Int.*,
476 vol. 1608, pp. 1–11, 2015.
- 477 [8] M. A. Ehyaei, P. Ahmadi, F. Atabi, M. R. Heibati, and M. Khorshidvand,
478 “Feasibility study of applying internal combustion engines in residential
479 buildings by exergy, economic and environmental analysis,” *Energy Build.*,
480 vol. 55, pp. 405–413, 2012.
- 481 [9] M. Özkan, D. B. Özkan, O. Özener, and H. Yılmaz, “Experimental study on
482 energy and exergy analyses of a diesel engine performed with multiple
483 injection strategies: Effect of pre-injection timing,” *Appl. Therm. Eng.*, vol.

- 484 53, no. 1, pp. 21–30, 2013.
- 485 [10] T. Morosuk, G. Tsatsaronis, and M. Schult, “Conventional and advanced
486 exergetic analyses: Theory and application,” *Arab. J. Sci. Eng.*, vol. 38, no.
487 2, pp. 395–404, 2013.
- 488 [11] M. Fallah, S. M. S. Mahmoudi, M. Yari, and R. Akbarpour Ghiasi,
489 “Advanced exergy analysis of the Kalina cycle applied for low temperature
490 enhanced geothermal system,” *Energy Convers. Manag.*, vol. 108, pp.
491 190–201, 2016.
- 492 [12] T. Morosuk and G. Tsatsaronis, “Advanced exergy analysis for chemically
493 reacting systems - Application to a simple open gas-turbine system,” *Int. J.*
494 *Thermodyn.*, vol. 12, no. 3, pp. 105–111, 2009.
- 495 [13] Y. Şöhret, E. Açıkkalp, A. Hepbasli, and T. H. Karakoc, “Advanced exergy
496 analysis of an aircraft gas turbine engine: Splitting exergy destructions into
497 parts,” *Energy*, vol. 90, 2015.
- 498 [14] F. Petrakopoulou, G. Tsatsaronis, T. Morosuk, and A. Carassai,
499 “Conventional and advanced exergetic analyses applied to a combined
500 cycle power plant,” *Energy*, vol. 41, no. 1, pp. 146–152, 2012.
- 501 [15] L. Wang, Y. Yang, T. Morosuk, and G. Tsatsaronis, “Advanced
502 thermodynamic analysis and evaluation of a supercritical power plant,”
503 *Energies*, vol. 5, no. 6, pp. 1850–1863, 2012.
- 504 [16] T. Morosuk and G. Tsatsaronis, “Advanced exergetic evaluation of
505 refrigeration machines using different working fluids,” *Energy*, vol. 34, no.
506 12, pp. 2248–2258, 2009.
- 507 [17] G. Tsatsaronis and T. Morosuk, “A general exergy-based method for
508 combining a cost analysis with an environmental impact analysis. Part I –
509 Theoretical Development,” *Asme Imece2008-67218*, p. 10, 2008.
- 510 [18] R. Lutz, P. Geskes, E. Pantow, and J. Eitel, “Use of Exhaust Gas Energy
511 in Heavy trucks using the rankine process,” *MTZ*, vol. 73, pp. 32–37, 2012.
- 512 [19] D. Seher, T. Lengenfelder, J. Gerhardt, N. Eisenmenger, M. Hackner, and
513 I. Krinn, “Waste Heat Recovery for Commercial Vehicles with a Rankine
514 Process,” *21 st Aachen Colloq. Automob. Engine Technol. 2012*, 2012.
- 515 [20] S. Kelly, G. Tsatsaronis, and T. Morosuk, “Advanced exergetic analysis:
516 Approaches for splitting the exergy destruction into endogenous and
517 exogenous parts,” *Energy*, vol. 34, no. 3, pp. 384–391, 2009.
- 518 [21] C. E. Campos Rodríguez, J. C. Escobar Palacio, O. J. Venturini, E. E. Silva
519 Lora, V. M. Cobas, D. Marques dos Santos, F. R. Lofrano Dotto, and V.
520 Gialluca, “Exergetic and economic comparison of ORC and Kalina cycle for
521 low temperature enhanced geothermal system in Brazil,” *Appl. Therm.*
522 *Eng.*, vol. 52, no. 1, pp. 109–119, 2013.
- 523 [22] G. Tsatsaronis and M. Park, “On avoidable and unavoidable exergy
524 destructions and investment costs in thermal systems,” *Energy Convers.*
525 *Manag.*, vol. 43, no. 9–12, pp. 1259–1270, 2002.
- 526 [23] J. Galindo, S. Ruiz, V. Dolz, L. Royo-Pascual, R. Haller, B. Nicolas, and Y.

- 527 Glavatskaya, "Experimental and thermodynamic analysis of a bottoming
528 Organic Rankine Cycle (ORC) of gasoline engine using swash-plate
529 expander," *Energy Convers. Manag.*, vol. 103, pp. 519–532, Oct. 2015.
- 530 [24] H. Kunte and J. Seume, "Partial Admission Impulse Turbine for Automotive
531 ORC Application," *SAE Tech. Pap.*, vol. 6, 2013.
- 532 [25] A. Keçebaş and H. Gökgedik, "Thermodynamic evaluation of a geothermal
533 power plant for advanced exergy analysis," *Energy*, vol. 88, pp. 746–755,
534 2015.
- 535 [26] Y.-R. Li, J.-N. Wang, and M.-T. Du, "Influence of coupled pinch point
536 temperature difference and evaporation temperature on performance of
537 organic Rankine cycle," *Energy*, vol. 42, no. 1, pp. 503–509, Jun. 2012.
- 538 [27] A. S. Panesar, R. E. Morgan, N. D. D. Miché, and M. R. Heikal, "Working
539 fluid selection for a subcritical bottoming cycle applied to a high exhaust
540 gas recirculation engine," *Energy*, vol. 60, pp. 388–400, 2013.
- 541 [28] T. Morosuk and G. Tsatsaronis, "Strengths and Limitations of Advanced
542 Exergetic Analyses," *Vol. 6B Energy*, no. November, p. V06BT07A026,
543 2013.
- 544